

Vibrational Spectra and Provisional Assignment of the $\Lambda(\delta\delta\delta)$ -Tris(1*S*,2*S*-cyclohexanediamine)iridium(III) Cation Spectra

G. BORCH,^a P. KLÆBOE^b and P. H. NIELSEN^c

^a Chemistry Department A, The Technical University of Denmark, DK-2800 Lyngby, Denmark, ^b Department of Chemistry, University of Oslo, Oslo 3, Norway and ^c Chemical Laboratory II, The H. C. Ørsted Institute, DK-2100 Copenhagen, Denmark

Dedicated to Jannik Bjerrum on the occasion of his 70th birthday

The infrared and Raman spectra of $\Lambda(\delta\delta\delta)$ -tris(1*S*,2*S*-cyclohexanediamine)iridium(III) chloride ($\Lambda\text{-chxn}_3\text{IrCl}_3$) and the corresponding *N*-deuterated compound (*N*-*d*₁₂- $\Lambda\text{-chxn}_3\text{IrCl}_3$) have been studied in the solid state and in aqueous solution in the region below 4000 cm⁻¹. Assuming *D*₃-symmetry of the complex ion, a provisional assignment of the fundamental vibrations of species *A*₁ and *A*₂ is given, based upon the Raman depolarisation ratios and the relative intensities of the infrared and Raman bands. The results of a vibrational analysis using a 54-parameter generalized valence force field (GVFF), partly transferred from cyclohexane and the tris(1,2-ethanediamine)rhodium(III) cation, support the assignments. A complete interpretation of the spectra including the fundamentals of species *E* is proposed on this basis. Certain remaining problems which will have to be clarified in future work are discussed.

The bidentate ligand 1*S*,2*S*-cyclohexanediamine (chxn) and its optical antipode are representatives of the substituted 1,2-ethanediamines. Several stereochemical studies of these compounds have appeared, notably Corey-Bailar¹ conformational analysis of five-membered chelate rings in metal complexes² and chiroptical studies^{3,4} correlating absolute configurations of analogous coordination compounds. Several crystal structures of such compounds are known⁵ and have given a basis for these correlations. Furthermore, the antitumor activity

of platinum(II) complexes with these ligands has been tested^{6,7} and it shows significant antileukemic activity. However, the vibrational spectra of chxn complexes are not known.

In previous papers^{8–10} the vibrational spectra of the $\Lambda(\delta\delta\delta)$ -tris(1,2-ethanediamine)rhodium(III) cation ($\Lambda\text{-en}_3\text{Rh(III)}$) were investigated. A normal coordinate analysis (NCA) of the parent ion and seven isotopically labelled species using a 38 parameter GVFF allowed an assignment of all the fundamental modes. The present study dealing with the $\Lambda(\delta\delta\delta)$ -tris(1*S*,2*S*-cyclohexanediamine)iridium(III) cation ($\Lambda\text{-chxn}_3\text{Ir(III)}$, Fig. 1) forms an extension of this work, but is more complex because of the larger ligands. Therefore, to test the application of the GVFF developed for $\Lambda\text{-en}_3\text{Rh(III)}$, this force field was combined with GVFF values for the cyclohexane ring. An NCA was derived for $\Lambda\text{-chxn}_3\text{-Ir(III)}$ based upon the most readily identified fundamentals of species *A*₁ and *A*₂. The results, together with the predicted fundamentals of species *E*, are presented in this paper.

STRUCTURE

Crystal structures of Ir(chxn)₃ complexes have not yet been determined by diffraction methods. Thus, symmetry and molecular parameters were transferred from analogous structures, e.g. the crystal

structure¹¹ of the congeneric $(-)_589\text{-}[\text{Co}(\text{+chxn})_3]\text{-Cl}_3$ pentahydrate. The complex ion in this compound has approximately D_3 -symmetry and the absolute configuration $\Lambda(\delta\delta\delta)$. The absolute configuration of the two carbon atoms in the ligand is S in agreement with a previous synthetic correlation³ and the cyclohexane rings have chair conformations. We have assumed that the preferred chair conformation of chxn in the complex ion is maintained in solution (*cf.* ^1H NMR evidence¹² that chair conformation with diequatorial position of the amino groups is also maintained in the free or substituted ligand in solution). Moreover, by using the method of "active racemates",¹³ Andersen *et al.*¹⁴ concluded from X-ray powder photographs that $(-)_589\text{-}[\text{Co}(\text{+chxn})_3]^{3+}$ and $(-)_589\text{-}[\text{Ir}(\text{+chxn})_3]^{3+}$ have the same absolute configuration, *viz.* $\Lambda(\delta\delta\delta)$. Hence the calculations in the present work have been based upon a $\Lambda(\delta\delta\delta)$ or $\Lambda(\text{le}l_3)$ structure assuming D_3 -symmetry (Fig. 1).

The technique for establishing the equilibrium configuration of the $\Lambda\text{-chxn}_3\text{Ir(III)}$ cation in cartesian coordinates was described previously.⁸ Since the octahedral radii of Ir^{3+} and Rh^{3+} are quite similar,¹⁵ the choice of bond distances and angles was based upon known structures of $\text{chxn}_3\text{Rh(III)}$ complexes^{16,17} (C–C: 1.53 Å, C–N: 1.48 Å, Rh–N: 2.08 Å, tetrahedral angles of the chxn ring). The N–Rh–N angles were chosen to be 87° .¹¹ Finally, the values C–H: 1.093 Å, N–H: 1.01 Å, H–C–H: $109^\circ 28'$, and H–N–H: 111° were

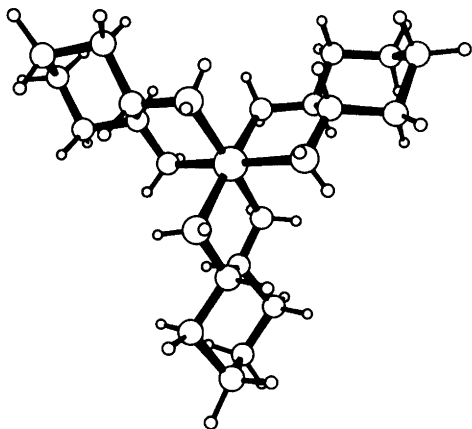


Fig. 1. The $\Lambda(\delta\delta\delta)$ -tris(1*S*,2*S*-cyclohexane("chair"))-diamine iridium(III) cation viewed along the trigonal axis.

chosen in agreement with previous calculations on tris(1,2-ethanediamine)rhodium(III) cation.⁸ We hope to improve these values in a forthcoming paper.

EXPERIMENTAL

$\Lambda\text{-chxn}_3\text{IrCl}_3\text{.aq}$ was prepared as described by Galsbøl.¹⁸ The analogous N -deuterated compound was obtained by dissolution in D_2O followed by evaporating the excess D_2O in a vacuum desiccator at room temperature. From spectra obtained in aqueous solution it appears that the exchange of hydrogen with deuterium at 20°C is complete within 6 h. The spectra of the corresponding anhydrous compounds were obtained by drying the alkali halide pellets at $100\text{--}150^\circ\text{C}$ over P_2O_5 *in vacuo* until no further changes could be observed in the spectrum (*ca.* 24 h). The pellets containing the anhydrous complex appear to be quite stable to the exposure of moisture from the air and we had no difficulties in obtaining reproducible spectra from different samples. However, the IR spectrum of $\Lambda\text{-chxn}_3\text{IrCl}_3\text{.aq}$ changed somewhat in the regions around 1600 and 820 cm^{-1} in different alkali halide discs and in Nujol mull as indicated by intervals in Table 2.

The instrumental equipment and techniques employed in observing the Raman and infrared spectra have been described elsewhere.⁹ In addition, some of the infrared spectra were recorded on a Perkin Elmer spectrophotometer 580 covering the region $4000\text{--}180\text{ cm}^{-1}$ and on a Bruker Model 114C fast scan Fourier transform spectrometer in the range $400\text{--}40\text{ cm}^{-1}$.

NORMAL COORDINATE ANALYSIS

The normal vibrations were calculated for the $\Lambda\text{-chxn}_3\text{Ir(III)}$ and $N\text{-}d_{12}\text{-}\Lambda\text{-chxn}_3\text{Ir(III)}$ cations as a full 67 body problem assuming D_3 symmetry. The 195 normal vibrations belong to the following irreducible representations: $33A_1(\text{R}) + 32A_2(\text{IR}) + 65E(\text{R,IR})$. The NCA was performed as described for the tris(1,2-ethanediamine)rhodium(III) cation.⁸ This paper should also be consulted for a description of the internal and symmetry coordinates and the initial force field which was transferred as far as possible in the present calculations. Additional information on the cyclohexane rings is available from the investigations of Wiberg and Shrake¹⁹ on cyclohexane and three deuterated species. Their procedure and final GVFF is compatible with ours,⁸ both based upon the method developed by

Snyder and Schachtschneider.²⁰ In order to preserve the transferability of the GVFF the symmetry coordinates used for the Λ -chxn₃Ir(III) cation were constructed to include all the local and cyclic redundancies ($14A_1 + 8A_2 + 22E$). These were eliminated automatically by the program during the calculations.

From the observed IR and Raman spectra it was possible to select many bands which would be ascribed as fundamentals of species A_1 and A_2 from the Raman depolarisation ratios or the IR and Raman band intensities. However, an exploratory NCA indicated the fundamentals of species E to overlap extensively those of species A_1 and A_2 . Therefore calculations on the A_1 and

A_2 blocks were done simultaneously until a satisfactory assignment was made. Using the converged GVFF the fundamentals of species E could be predicted and compared with the experimental results. Provided all the remaining relatively strong bands could be assigned to species E by this procedure, the NCA was considered satisfactory. Only those force constants which appeared necessary to ensure a reasonable good fit between the observed and calculated frequencies were included in the iterative procedure. The remaining force constants were fixed at the values obtained previously.^{8,19} By allowing the 35 force constants listed in Table 1 to vary, a rapid convergence was ensured with a standard error between the observed and calculated frequencies of less than 0.75 % for each of the four blocks considered, (A_1 and A_2 for Λ -chxn₃Ir(III) and N - $d_{1,2}$ - Λ -chxn₃Ir(III)). The calculated frequencies with approximate descriptions are listed together with the observed frequencies in Tables 2 and 3, which also include the tentative assignments of the fundamentals of species E .

Despite the limitations imposed on the calculations the final force field (Table 1) falls within the range of known values from related molecules. We consider first the force constants related to the chelate rings listed in the first column of Table 1. By analogy to complex formation with NH_3 , the replacement of Rh(III) with Ir(III) is predicted²¹ to increase the strength of the metal-ligand bond. Thus, the corresponding stretching force constants, K_L , increases from 1.607 mdyn/Å in the tris(1,2-ethanediamine)Rh(III) cation⁸ to 1.906 mdyn/Å in the Λ -chxn₃Ir(III) cation. The corresponding increase in H_ω (0.76 \rightarrow 1.57 mdyn Å/(rad)²) and $F_{L\omega}$ (0.22 \rightarrow 0.63 mdyn Å/(rad)²) indicate an increased resistance to bending of the metal-N-C angle (ω). On the other hand, the added electron density in the metal-ligand bond should be followed by a decrease in the donor part of the ligand. It is satisfactory, therefore, that the force constants pertaining to the C-NH₂ group (H_α , H_β , K_d , K_D) all decrease from the Rh(III) to the Ir(III) complex. The force constants of the cyclohexane ligand rings (listed in the second column of Table 1) cannot be directly compared with those of cyclohexane.¹⁹ The changes caused by substitution with the amino groups are uncertain, and the NH₂-CH-CH-NH₂ moiety has been treated as part of the chelate,⁸ while the remaining part of the cyclohexane rings has been treated according to Ref. 19. However, the substantial increase in the force

Table 1. The final valence force constants for the Λ -chxn₃Ir(III) cation.^a

Symbol according to Ref. 8	Value ^b	Symbol according to Ref. 19	Value ^b
K_r	4.739	K_R	4.138
K_d	5.354	H_ω	1.255
K_R	4.408	H_r	0.202
K_D	3.722	K_d	4.570
K_L	1.906	H_γ	0.681
F_d	0.107	H_δ	0.537
F_{LL}	0.188	F_R	0.236
F'_{LL}	-0.08	$F_{R\omega}$	0.441
H_α	0.519	$F_{R\gamma}$	0.301
H_c	0.745		
H_γ	0.712		
H_ψ	0.493		
H_β	0.436		
H_ω	1.571		
$H_\phi = H_\theta$	1.150		
H_η	0.664		
$F_{R\psi}$	0.318		
$F_{D\gamma}$	0.380		
$F_{D\psi}$	0.435		
$F_{L\omega}$	0.629		
F_γ	-0.169		
F_β	0.089		
$F_\phi = F_\theta$	-0.266		
$F'_\phi = F'_\theta$	0.074		
H_r	0.246		
H_Δ	0.161		

^a All other valence force constants were transferred from Refs. 8 and 19. ^b In units of mdyn/Å (stretch constants); mdyn/rad (stretch-bend interaction constants) and mdyn Å/(rad)² (bending and torsion constants).

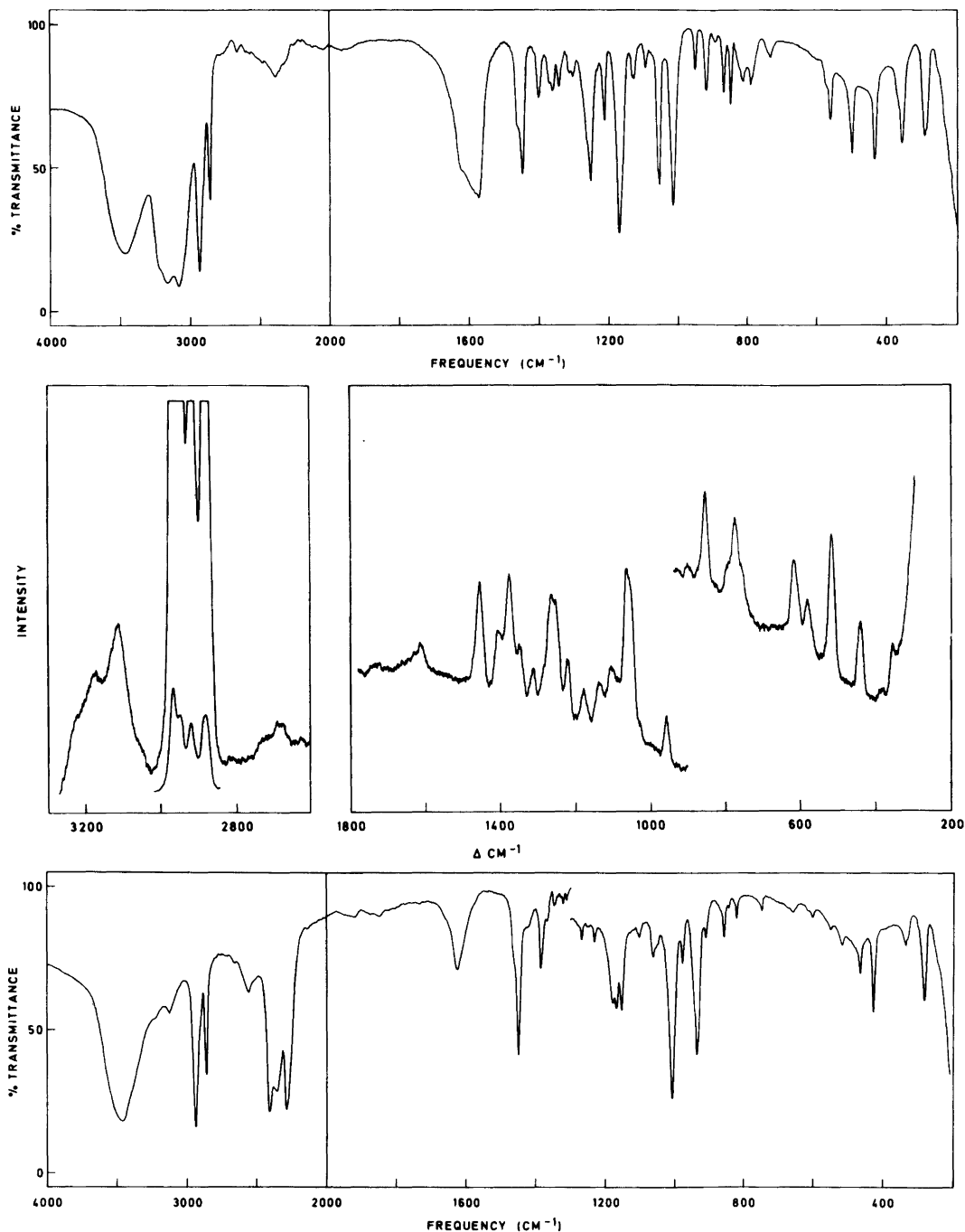


Fig. 2. The infrared (top, KI pellet) and Raman (middle, solid) spectra of $\Lambda(\delta\delta\delta)$ -tris(1*S*,2*S*-cyclohexanediamine)iridium(III) cation and the infrared (bottom, KI pellet) spectrum of the corresponding N - d_{12} species. The water peaks at 3460 and 1625 cm⁻¹ in the bottom spectrum were caused by humidity in the KI.

constant for C-C-C bending (H_{cc} , $1.08 \rightarrow 1.26$ mdyn $\text{\AA}/(\text{rad})^2$) from cyclohexane to the chxn ligand may be explained by an increased stiffness of the cyclohexane ring when involved in chelate formation.

RESULTS AND DISCUSSION

The IR and Raman spectra of Λ -chxn₃IrCl₃.aq and the IR spectrum of N -d₁₂- Λ -chxn₃IrCl₃.aq are shown in Fig. 2. The observed frequencies of the parent compound are listed in Table 2, which includes a full assignment and description of the

Table 2. Observed and calculated (calc) vibrational frequencies (cm^{-1}) of the $\Lambda(\delta\delta\delta)$ -tris(1,2-cyclohexanediamine)iridium(III) cation with tentative assignments of the spectra and description of the fundamentals.

Infrared ^a			Raman ^{a,b}			Calc ^c	Assignment and description ^d (PED, %)	Predicted for species E ^d
Solid hydrate	Solid anhydrous	Solution H ₂ O	Solid hydrate	Solution H ₂ O	Polarization			
3460s, br				3405s, br			H ₂ O	
3240s, br	3205vs	3210s, br	3225m, br, sh	3255s, br		{3185 3185	ν_{31}^a , ν_{32}^a , ν_{33}^a NH ₂ (99) ν_{34}^a , ν_{35}^a NH ₂ (99)	} $\nu_{66}-\nu_{69}$, ν NH ₂
3170vs, br	3170vs, sh	3160s, sh	3160m, br			{3144 3142	ν_{36}^a , ν_{37}^a , ν_{38}^a NH ₂ (99) ν_{39}^a , ν_{40}^a NH ₂ (99)	
		3120s, sh	3120m, sh					
3070vs, br			3105m, br					
			2955vs	2956vs	0.35	2958	ν_{31}^a , ν CH (96)	} $\nu_{70}-\nu_{79}$, ν CH
2950s, sh	2960s	2951s				2948	ν_{36}^a , ν CH (98)	
2935vs	2935s, sh	2936m, sh	2934s	2935s, sh	D?	2932	ν_{36}^a , ν CH (98)	
2922s, sh			2920w, sh			{2925 2923	ν_{37}^a , ν CH (99) ν_{38}^a , ν CH (100)	
2908m, sh	2905s, sh	2912w, sh	2907s	2915s	0.3	2923	ν_{35}^a , ν CH (99)	
			2897w, sh					
			2872s	2876s	0.15	{2870 2868	ν_{66}^a , ν CH (99) ν_{71}^a , ν CH (99)	
2868m, sh	2865s	2872m				{2868 2867	ν_{39}^a , ν CH (99) ν_{40}^a , ν CH (99)	
2858s		2862w, sh	2862m, sh					
1625s, sh			1629w, sh	1630s, br			H ₂ O	
	1600s	1608w, sh	1608m, br			{1605 1600	ν_{80}^a , δ NH ₂ (95) ν_{81}^a , δ NH ₂ (96)	} ν_{80} , ν_{81} , δ NH ₂
1570-1602vs		1591m, br	1581w, sh				H ₂ O	
1473w, sh	1470m	1473w, sh	1477w, sh	1474vw, sh	D?			1479, ν_{82} , δ CH ₂ (97)
1464s	1465s	1467m	1466m	1467w, sh	D?	{1467 1467	ν_{83}^a , δ CH ₂ (100) ν_{84}^a , δ CH ₂ (100)	1467, ν_{83} , δ CH ₂ (99)
1456s, sh	1449m							
1449s	1442s	1454s	1451s	1454s	D	{1454 1453	ν_{10}^a , δ CH ₂ (97) ν_{11}^a , δ CH ₂ (99)	{1454, ν_{84} , δ CH ₂ (100) 1453, ν_{85} , δ CH ₂ (100)
			1402m	1404m	0.65	1409	ν_{11}^a , chx (58), ν NH ₂ (26)	} $\nu_{86}-\nu_{94}$, chx, ν NH ₂
1402m	1392m	1405m				1396	ν_{14}^a , chx (70), ν NH ₂ (30)	
1390vw			1390w, sh	1391w, sh	D			
1370m, sh	1372w	1373w	1374s	1374s	0.5	1370	ν_{12}^a , chx (59), ν NH ₂ (24)	
1363m	1357m	1363vw	1363w, sh	1368w, sh		1351	ν_{15}^a , chx (99)	
			1346m	1351m	0.65	1340	ν_{13}^a , chx (80), ν NH ₂ (23)	
1345m	1349m	1348m				1336	ν_{16}^a , chx (69), ν NH ₂ (36)	
1336w, sh	1341w, sh	1340w, sh	1336vw, sh	1340vw, sh				
1313w		1317vw	1314w	1315vw	D?	1324	ν_{14}^a , chx (100)	
1305w	1304m		1308w	1305vw	D?			
1300w	1298w, sh					1281	ν_{12}^a , chx (80), ν NH ₂ (18)	} $\nu_{86}-\nu_{94}$, chx, ν NH ₂
			1283w, br, sh	1283w, sh		1278	ν_{15}^a , chx (88)	
1264w, sh	1270m, sh	1272w, sh	1263vs	1264vs	P?	1266	ν_{16}^a , chx (100)	1265, ν_{95} , chx (100)
1253s	1253vs	1261s	1248vs	1247s	D			1260, ν_{96} , ν NH ₂ (75)
1234w	1238w, sh	1243w, sh	1239w, sh	1237w, sh		1234	ν_{18}^a , chx (90)	1232, ν_{97} , chx (94)
1220w, sh			1227w, sh	1226w, sh				

Table 2. Continued.

Infrared ^a			Raman ^{a,b}			Calc ^c	Assignment and description ^d (PED, %)	Predicted for species E ^d
Solid hydrate	Solid anhydrous	Solution H ₂ O	Solid hydrate	Solution H ₂ O	Polarization			
1215m	1215m	1218m	1220s	1220m	P?	1218	ν_{17a_1} , ωNH_2 (57), chx (32)	} $\nu_{98}-\nu_{101}$, chx, ωNH_2
			1189w,sh	1185w	0.5	1218	ν_{9a_2} , ωNH_2 (56), chx (44)	
1171vs	1164vs	1173vs	1175m,br	1175w,br	D?	1189	ν_{18a_1} , chx (69), ωNH_2 (27)	
1160m,sh		1157w,sh	1152w	1152vw		1162	ν_{50a_2} , chx (84), ωNH_2 (13)	
1134w	1134w,sh	1135w	1137m	1137m	1132w	D?	ν_{51a_2} , chx (90), ωNH_2 (16)	1148, ν_{102} , νCN (25), chx (49)
1130w	1129w	1126vw						
		1110vw	1112w,sh					
1097w	1095w	1095w	1107m	1097m	0.1	1121	ν_{19a_1} , chx (67), νCN (19)	
1080w	1075w	1082vw	1080vw?	1084w,sh	P?			
1062s,sh		1066m,sh	1062vs	1067vs	D?	1066	ν_{52a_2} , chx (59), νCN (40)	
1057s	1057vs	1061s	1049vs	1056vs	D	1049	ν_{20a_1} , chx (97)	1052, ν_{103} , chx (88), νCN (14)
	1032vw,sh		1026w	1034vw		1038	ν_{21a_1} , chx (90), νCN (16)	} $\nu_{104}-\nu_{106}$, chx, νCN
1017vs	1023vs	1020vs	1013vw	1020vw	D?	{1022 1011	ν_{22a_1} , chx (51), νCN (46) ν_{53a_2} , chx (53), νCN (49)	
954m	953m		955m	956m	D			970, ν_{107} , νCN (54), chx (49)
921m	921s		922vw	922vw		{929 922	ν_{54a_2} , chx (100) ν_{23a_1} , chx (92)	{928, ν_{108} , chx (81) 920, ν_{109} , chx (92), νCN (13)
900w,sh	900w		900w	901w	D			
891w	890w		890vw	895vw		887	ν_{55a_2} , chx (100)	885, ν_{110} , chx (100)
871m	868s		871vw	870w,sh	D?	867	ν_{56a_2} , chx (87)	
851m	850m		852s	855s	0.14	851	ν_{24a_1} , chx (98)	ν_{111} , ν_{112} , chx
	829s							
813-823m	822s							
			790m	792m	P?	799	ν_{25a_1} , chx (67), ωNH_2 (28)	} $\nu_{113}-\nu_{115}$, ωNH_2 , chx
792m	791m					786	ν_{57a_2} , ωNH_2 (89)	
769vvw	763w,sh		772s	762s	0.1	760	ν_{26a_1} , ωNH_2 (58), chx (36)	
748vvw	745w		756m	750w,sh	P?			
737vw,br	730vw,sh		740w,sh					
				655vw	P			
650vvw			645vw,br	640vw				
620vw	618w		614m	619s	0.3	{629 614	ν_{27a_1} , $\nu_{8a}\text{IrN}$ (72), δchel (38) ν_{58a_2} , chx (85)	629, ν_{116} , $\nu_{8a}\text{IrN}$ (70)
605vvw	608vw		603w,sh	606w,sh	D?			600, ν_{117} , chx (84)
579m,sh	579m		578m	580m	D	583	ν_{59a_2} , $\nu_{8a}\text{IrN}$ (67), δchel (41)	588, ν_{118} , chx (46), δchel (23)
567m	565m		565w	567w,sh	D			
552vw,sh			540vw	545vvw		558	ν_{28a_1} , chx (53), δchel (27)	
	530w,sh		528w	527vw,sh	P?			
515m,sh								
508s	505s		514vs	503vs	0.17	502	ν_{29a_1} , chx (86)	{505, ν_{119} , chx (83) 490, ν_{120} , δchel (57)
				470vw	P			
	460vw,sh		460vvw	452vw,sh	D	453	ν_{60a_2} , chx (83)	
437s	437s		436s	438s	D			418, ν_{121} , chx (65), $\nu_{8a}\text{IrN}$ (27)
420vw	422vw			425w,sh				
			398vw					

Table 2. Continued.

Solid hydrate	Infrared ^a		Raman ^{a,b}			Calc ^c	Assignment and description ^d (PED, %)	Predicted for species E
	Solid anhydrous	Solution H ₂ O	Solid hydrate	Solution H ₂ O	Polarisation			
375s	375m, sh		382w	385vw		388	$\nu_{61}^{a_2}$, chx(58), δ_{chel} (17)	385, ν_{122} , chx(38), δ_{chel} (38)
362s	366s 360s, sh		360w	365vw		358	$\nu_{30}^{a_1}$, chx(88)	357, ν_{123} , chx(91)
337w, sh	339w		335w, br	340vw				
303s	300s		313w	312w	D			316, ν_{124} , δ_{chel} (43), chx(25)
291s	292s			290vw	D	285	$\nu_{62}^{a_2}$, δ_{chel} (54), chx(30)	
264m	258m, sh		260vw	266vw	D?	268	$\nu_{31}^{a_1}$, δ_{chel} (96)	270, ν_{125} , δ_{chel} (35), chx(30)
241m	241m, sh			240rvw	D?	233	$\nu_{63}^{a_2}$, δ_{chel} (35), chx(32)	
230m	232m 216vw, sh 200vw, sh		233w, sh	230w 211w	D D?			224, ν_{126} , δ_{chel} (45), chx(32)
173s			198m	198m	0.15	199	$\nu_{32}^{a_1}$, δ_{chel} (56), $\nu_{\text{as}}^{\text{IrN}}$ (17)	195, ν_{127} , $\nu_{\text{as}}^{\text{IrN}}$ (38)
158m, sh			156vw	162vw				165, ν_{128} , δ_{chel} (42), chx(41)
132s			132vw	130vw		130	$\nu_{64}^{a_2}$, δ_{chel} (77)	
118m, sh				118vw				
97w, sh						95	$\nu_{33}^{a_1}$, δ_{chel} (45), chx(35)	
80w, sh						45	$\nu_{65}^{a_2}$, δ_{chel} (92)	84, ν_{129} , δ_{chel} (64) 37, ν_{130} , δ_{chel} (50), $\nu_{\text{as}}^{\text{IrN}}$ (39)

^a The following abbreviations have been used: s, strong; m, medium; w, weak; br, broad; sh, shoulder. Weak bands in the region between 1600 and 4000 cm^{-1} have been omitted.

^b The depolarisation ratios are given in cases where they can be accurately determined ($\rho = 0.75$ corresponds to a fully depolarised band). In other cases the following abbreviations have been used: D = depolarised; P, polarised.

^c Iteration based upon species A_1 and A_2 of $\Lambda\text{-chxn}_3\text{IrCl}_3$ and $N\text{-d}_{12}\text{-}\Lambda\text{-chxn}_3\text{IrCl}_3$.

^d Abbreviations: ν = stretching; δ = deformation; ρ = rocking; t = twisting; τ = torsion; chel = vibrations of the chelate ring; chx = vibrations of the cyclohexane ring including hydrogen atoms, and, as subscripts, s = symmetric, and as = antisymmetric. The potential energy distribution (PED, $\sum_{ik} 100E_{1i}E_{1k}^2/\sum_k$) is stated only for significant contributions.

fundamentals of species A_1 and A_2 together with the calculated values. In the last column of Table 2, the main features of the fundamentals predicted for species E are summarized. Quite similar data are given for $N\text{-d}_{12}\text{-}\Lambda\text{-chxn}_3\text{IrCl}_3$ in Table 3.

The spectra of $\Lambda\text{-chxn}_3\text{IrCl}_3$ exhibit two strong and broad bands at 3205–3255 cm^{-1} and 3160–3170 cm^{-1} due to the antisymmetric and symmetric NH_2 stretching modes, respectively. The corresponding ND_2 stretching modes are observed in the region 2200–2400 cm^{-1} . As anticipated, the appearance of the CH stretching region between 2850 and 3000 cm^{-1} is almost identical in the spectra of the parent (Table 2) and N -deuterated (Table 3) molecules. The four strong, polarised bands observed in the Raman spectra near 2955, 2935, 2915 and 2875 cm^{-1} supposedly originate from the fundamentals $\nu_3 - \nu_7(a_1)$ with overlap between ν_6 and ν_7 . Corresponding bands in the spectrum of

cyclohexane¹⁹ are found in the range 2936–2853 cm^{-1} . Our NCA reveals that ν_3 near 2955 cm^{-1} is due to CH stretching of the $>\text{CH}-\text{NH}_2$ groups, while the remaining fundamentals in the range 2935–2875 cm^{-1} correspond to stretching of the $>\text{CH}_2$ groups.

The NH_2 scissors are all assigned to the band near 1600 cm^{-1} , partly obscured by bands due to water occurring in the region 1570–1630 cm^{-1} . Complete deuteration shifts this mode to ca. 1210 cm^{-1} which is close to the strong broad D_2O band at 1200 cm^{-1} . The NH_2 twisting and wagging modes are assigned to bands in the 1340–1410 cm^{-1} and 1150–1260 cm^{-1} regions, respectively. The corresponding ND_2 modes are coupled extensively with each other and with vibrations of chxn , and occur in the region 850–1160 cm^{-1} . The NH_2 and ND_2 rocking modes are found at 760–800 and 590–635 cm^{-1} , respectively.

Table 3. Observed and calculated (calc) vibrational frequencies (cm^{-1}) of the *N*-perdeuterio- $\Delta(\delta\delta\delta)$ -tris(1,2-cyclohexanediamine)iridium(III) cation with tentative assignments of the spectra and description of the fundamentals.

Solid hydrate	Infrared ^a		Raman ^{a,b}			Calc ^c	Assignment and description ^d (PED, %)	Predicted for species E ^d
	Solid anhydrous	Solution D ₂ O	Solid hydrate	Solution D ₂ O	Polarization			
2954s, sh	2958m, sh	2950s	2957vs	2956vs	0.25	2958	ν_{1a_1} , ν_{CH} (96)	} $\nu_{66}-\nu_{75}$, ν_{CH}
2939s	2939s, sh	2940s, sh	2940vs	2938m	D?	2948	ν_{34a_2} , ν_{CH} (98)	
2924s, sh	2924s					{2925	ν_{3c_2} , ν_{CH} (99)	
2908m, sh	2908m, sh	2912m, sh	2908s	2914s	0.2	2923	ν_{3a_1} , ν_{CH} (99)	
			2872vs	2873vs	0.1	{2870	ν_{5a_1} , ν_{CH} (99)	
						{2868	ν_{5a_1} , ν_{CH} (99)	
2863s	2860a	2872m				{2868	ν_{37a_2} , ν_{CH} (99)	
						{2867	ν_{38a_2} , ν_{CH} (99)	
2405s						2404	ν_{6a_1} , ν_{ND_2} (97)	
2364s, br	2378s		2368m			2403	ν_{39a_2} , ν_{ND_2} (98)	
2330w, sh	2330s, sh							} $\nu_{76}-\nu_{79}$, ν_{ND_2}
2273s	2280s, sh		2286m			{2311	ν_{4a_1} , ν_{ND_2} (97)	
	2240vs					{2307	ν_{40a_2} , ν_{ND_2} (97)	
1475w, sh	1468m, sh		1475w, sh					} 1479, ν_{80} , δ_{CH_2} (98)
			1466m, sh	1467w	P	1467	ν_{8a_1} , δ_{CH_2} (100)	
1465m, sh	1463s	1462m, sh				1467	ν_{41a_2} , δ_{CH_2} (100)	} $\nu_{81}-\nu_{83}$, δ_{CH_2} (100)
1452s	1446m	1453s	1450s	1452vs	D?	{1453	ν_{4a_1} , δ_{CH_2} (99)	
						{1453	ν_{42a_2} , δ_{CH_2} (100)	
1431m, sh	1438s	1436m, sh						} $\nu_{84}-\nu_{90}$, chx
1420w, sh	1420w, sh	1419w, sh	1419vw					
1386m	1475m	1385m	1379s	1386s	0.7	1384	ν_{10a_1} , chx (99)	
1370w, sh		1362w	1368m, sh	1368m	D	1373	ν_{43a_2} , chx (100)	
1347w	1345w	1349w	1343w	1348w	0.7	{1353	ν_{11a_1} , chx (100)	
						{1349	ν_{44a_2} , chx (100)	
1325w	1327w	1327w	1325w	1328w	0.3	1325	ν_{12a_1} , chx (100)	
1305w	1302m	1305w	1306w	1306w	D	{1299	ν_{45a_2} , chx (100)	
						{1293	ν_{13a_1} , chx (96)	
1269w	1275w	1265w	1267w, sh	1268w, sh		1266	ν_{14a_1} , chx (100)	
1251vw	1248w		1248s	1253s	D			} 1264, ν_{91} , chx (100)
1225w	1226w		1228s	1230s	D	1235	ν_{46a_2} , chx (99)	
1209vw	1202w		1206vw	1210m, sh		{1215	ν_{15a_1} , δ_{ND_2} (76)	} $\nu_{92}-\nu_{98}$, chx, δ_{ND_2}
						{1208	ν_{17a_2} , chx (73), δ_{ND_2} (22)	
						{1207	ν_{16a_1} , chx (88)	
						{1204	ν_{48a_2} , δ_{ND_2} (61), chx (30)	
		1200s, br	1200s, br	1200s, br	P		D ₂ O	
			1190w	1190w				
1178m	1185m, sh		1183w	1185w				
1171m	1177m	1167w, sh				1166	ν_{49a_2} , chx (100)	
1155m	1152m	1150w	1158s	1159vs	0.5	1147	ν_{17a_1} , chx (65), ν_{ND_2} (14)	
1125w, sh	1124w							
1120w	1116w	1129vw	1133vw	1133vw				
1100w	1098w	1102w	1099w, br	1102m	0.5	1095	ν_{18a_1} , chx (89)	
1064m	1061m	1065w	1068s	1070s	D	1066	ν_{50a_2} , chx (65), ν_{CN} (34)	
1052m	1047m	1055w	1054s, sh	1057s, sh	D	1050	ν_{19a_1} , ν_{CN} (69), ν_{ND_2} (30)	

Table 3. Continued.

Infrared ^a			Raman ^{a,b}			Calc ^c	Assignment and description ^d (PED, %)	Predicted for species E ^d
Solid hydrate	Solid anhydrous	Solution D ₂ O	Solid hydrate	Solution D ₂ O	Polarization			
1030m, sh	1033s, sh		1032vw	1025vw, br	P?	1042	ν_{20}^a , chx(97)	1038, ν_{102} , chx(100)
1008s	1015vs	1010s	1022vw			1022	ν_{51}^a , ν_{CN} (52), t/ ν_{ND_2} (31)	} ν_{103}^a - ν_{110} , chx, ν_{CN} , ν_{ND_2}
			999vw			1000	ν_{21}^a , chx(90), t/ ν_{ND_2} (22)	
980m	972m		980vvw			983	ν_{52}^a , t/ ν_{ND_2} (52), chx(32)	
945m, sh	944m, sh		945vw	950w	O.7	945	ν_{53}^a , ν_{ND_2} (54)	
934s	932s		928m	928m	O.7	925	ν_{22}^a , ν_{ND_2} (37), chx(35)	
913m	922s		914vw, sh	914w	O.7	917	ν_{54}^a , chx(88)	
	910m, sh							
878w	876m		889w	880w	D?	878	ν_{55}^a , chx(94)	
860m	860w, sh		856m, sh	862vw	D?	{859 856	ν_{53}^a , chx(72), t/ ν_{ND_2} (25) ν_{56}^a , chx(76)	851, ν_{111} , chx(81)
	852w							
846w	844m		848s	848vs	O.12	841	ν_{24}^a , chx(90)	846, ν_{112} , chx(80)
824m	827w			823vw	D?			
	774w, sh							
760m	765m		767s	765vs	O.2	768	ν_{25}^a , chx(78), ν_{ND_2} (13)	764, ν_{113} , chx(79), ν_{ND_2} (13)
	756w, sh			755m, sh	D			
	720m, sh		720vw	720vw				
709w	712m							
680w	682m		677vw, br	679vw				
668vw, sh	650vw			667vw	D?			
				642vw, sh	P			
			635w, br	628w				633, ν_{114} , ν_{ND_2} (72)
612vw	613w			620w		624	ν_{57}^a , ν_{ND_2} (60)	
			600vw, sh	606w	P	611	ν_{26}^a , ν_{ND_2} (73)	
	593vw, sh		590w, sh	590w, sh		599	ν_{58}^a , chx(68), ν_{ND_2} (22)	{600, ν_{115} , ν_{ND_2} (74) 595, ν_{116} , chx(98)
573w, sh	575w, sh		577m	574s	O.15	557	ν_{27}^a , ν_{IrN} (54), δ_{chel} (47)	
552m	555m		552w	552w	D			557, ν_{117} , ν_{IrN} (34), δ_{chel} (43)
	534w, sh							
528m	528m		523w	530vw	D	527	ν_{59}^a , ν_{IrN} (49), δ_{chel} (44)	527, ν_{118} , chx(34), ν_{ND_2} (22)
500vw	504w			499w, sh		518	ν_{28}^a , chx(40), ν_{ND_2} (15)	
483m, sh	487m		481s	480vs	O.13	495	ν_{29}^a , chx(77), ν_{IrN} (11)	496, ν_{119} , chx(71), ν_{IrN} (16)
468m	474s			470m, sh	D			475, ν_{120} , δ_{chel} (53), chx(45)
457w, sh								
451vw, sh			455w	445w	D			
429s	432s		427s	426s	D	437	ν_{60}^a , chx(72), ν_{IrN} (20)	393, ν_{121} , chx(53), ν_{IrN} (30)
422m, sh	422m, sh							
412w, sh			408vw	405vw	D?			
346m, sh	350m, sh		357vw	365vw		{363 353	ν_{61}^a , chx(73) ν_{30}^a , chx(96)	354, ν_{122} , chx(46), ν_{IrN} (17)
338m	341m		335vw	335vw				351, ν_{123} , chx(94)
	336m, sh							
292s								
284s	285s		283vw					288, ν_{124} , δ_{chel} (44)
242m	250m					257	ν_{62}^a , δ_{chel} (64)	260, ν_{125} , δ_{chel} (33), chx(27)

Table 3. Continued.

Infrared ^a			Raman ^{a,b}			Calc ^c	Assignment and description ^d (PED, %)	Predicted for species E ^d
Solid hydrate	Solid anhydrous	Solution D ₂ O	Solid hydrate	Solution D ₂ O	Polarization			
			239w	239w		232	$\nu_{31}^{a_1}$, δ_{chel} (78)	
237m						228	$\nu_{63}^{a_2}$, chx (39), δ_{chel} (26)	
			220vw	219vw	D?			206, ν_{126} , δ_{chel} (46), ν_{IrN} (23)
			193w	196m	0.17	194	$\nu_{32}^{a_1}$, δ_{chel} (71)	187, ν_{127} , δ_{chel} (39), ν_{IrN} (20)
171s								
156m				160w, br	D			161, ν_{128} , δ_{chel} (43), chx (41)
134m, sh				128vw		126	$\nu_{64}^{a_2}$, chel (82)	
116s				116vw				
96m, sh						94	$\nu_{33}^{a_1}$, δ_{chel} (47), chx (46)	
77w, sh								83, ν_{129} , δ_{chel} (67), chx (26)
						45	$\nu_{65}^{a_2}$, δ_{chel} (93)	36, ν_{130} , δ_{chel} (49), ν_{IrN} (39)

^{a,b,c,d} see footnotes to Table 2.

Between 810 and 830 cm^{-1} in the spectrum of $\Lambda\text{-chxn}_3\text{Ir(III)}$ and between 680 and 720 cm^{-1} in the spectrum of $N\text{-}d_{12}\text{-}\Lambda\text{-chxn}_3\text{Ir(III)}$, 2–3 rather strong bands are observed in the IR spectra without, or with very weak counterparts in the Raman spectra. These bands are very sensitive to the state of hydration of the complex compound. The NCA predicts no bands in this region, and we cannot at present give any explanation of their origin. Provided the strong, polarized Raman line at 762 cm^{-1} in the spectrum of $\Lambda\text{-chxn}_3\text{Ir(III)}$ has been correctly assigned, it appears improbable that they are due to rocking modes of the amino groups. If these bands should be dependent on the anion, they might arise from N–(H)–Cl stretching (*cf.* the ethylenediammonium halides²²).

The vibrations of the cyclohexane ring (chxn) are difficult to describe in simple terms, but the gross features are quite similar to those for cyclohexane.¹⁹ According to the NCA the CCH deformation vibrations of the $>\text{CH}-\text{CH}<$ group give rise to the bands between 1350 and 1410 cm^{-1} . The CN stretching modes should contribute heavily to the bands found in the 1020–1070 cm^{-1} range in agreement with the corresponding bands in $\Lambda\text{-en}_3\text{Rh(III)}$, calculated to occur near 1030 and 1060 cm^{-1} .⁸

In the region below 700 cm^{-1} , the three strong, polarized Raman lines at 619, 503, and 198 cm^{-1} in the spectrum of $\Lambda\text{-chxn}_3\text{IrCl}_3$ must be assigned to fundamentals of species A_1 . In the spectrum of $N\text{-}d_{12}\text{-}\Lambda\text{-chxn}_3\text{IrCl}_3$ they occur at 574, 480 and 196 cm^{-1} , respectively. However, according to the

NCA, the deuteration shift of the band mainly involving symmetric Ir–N stretching should be almost 75 cm^{-1} while the highest shift observed is 619–574=45 cm^{-1} . All attempts to obtain agreement between the observed and calculated shifts, *e.g.* by introducing different assignments and various interaction force constants, were unsuccessful.

Although the spectra of 1,2-ethanediamine complexes of Ir(III) and Rh(III) are generally very similar²³ the symmetric metal-nitrogen stretching mode is expected at higher frequencies in the iridium than in the rhodium complex.²⁴ We assigned the Raman lines at 619/574 cm^{-1} to $\nu_2(a_1)$ since the force field indicated a substantial contribution of $\nu_3\text{IrN}$ to this band. However, this assignment leads to the surprising result (Tables 2 and 3) that the strongest Raman bands at 503/480 cm^{-1} should originate in a deformational vibration of the cyclohexane ring. This appears surprising since in cyclohexane (D_{3d} -symmetry) the ring bending modes have²⁵ low intensities. In the complex ion with local C_2 -symmetry of the ligands and an overall D_3 -symmetry, a strong induced transition dipole moment parallel to the C_3 axis would be expected for a collective motion of the six carbon atoms of the ligands (*cf.* Fig. 1), thus producing a strong Raman band. On the other hand, the calculated shift on deuteration is only 7 cm^{-1} in contrast to the experimental value of 23 cm^{-1} . Without ¹⁵N substitution, which would locate the $\nu_3\text{IrN}$ vibration with certainty,⁹ it is at present not possible to solve this problem unambiguously.

In the case of $\Lambda\text{-en}_3\text{RhCl}_3$ the Rh–N stretching

frequencies⁸⁻¹⁰ are found in the order $\nu_s \text{RhN}(A_1) > \nu_{as} \text{RhN}(E) > \nu_{as} \text{RhN}(A_2)$, while the corresponding Ir-N stretching frequencies of Tables 2 and 3 follow the order $\nu_s \text{IrN}(A_1)$ at 619 cm^{-1} , $\nu_{as} \text{IrN}(E)$ also at 619 cm^{-1} , and $\nu_{as} \text{IrN}(A_2)$ at 580 cm^{-1} . From Table 2 it can be seen, that the band near 580 cm^{-1} is strong both in IR and in Raman and should rather be assigned as $\nu_{as} \text{IrN}(E)$. The band at 565 cm^{-1} , strong in the IR, but weak in the Raman spectrum, might be assigned to $\nu_{as} \text{IrN}(A_2)$. However, if this alternative is adopted, it appears impossible to obtain a reasonable assignment of the corresponding bands in the spectra of $N\text{-}d_{1,2}\text{-}\Lambda\text{-chxn}_3\text{IrCl}_3$ compatible with the NCA. An explanation must wait for an unambiguous identification of $\nu_s \text{IrN}$ as discussed above.

Acknowledgements. The authors are indebted to Dr. F. Galsbøl for making available some results prior to publication and for supplying a sample of the title compound, and to Mrs. J. E. Gustavsen for recording some of the spectra. Financial support from the Danish Natural Science Research Council and the Norwegian Research Council for Science and the Humanities is acknowledged.

REFERENCES

1. Corey, E. J. and Bailar, J. C., Jr. *J. Am. Chem. Soc.* 81 (1959) 2620.
2. Harnung, S. E., Sørensen, B. S., Creaser, I., Maegaard, H., Pfenninger, U. and Schäffer, C. E. *Inorg. Chem.* 15 (1976) 2123.
3. Woldbye, F. *Rec. Chem. Prog.* 24 (1963) 197.
4. Woldbye, F. *Studier over optisk aktivitet*, Polyteknisk Forlag, Copenhagen 1969, p. 189.
5. Saito, Y. *Coord. Chem. Rev.* 13 (1974) 305.
6. Meichen, S. J., Gale, G. R., Walker, E. M., Atkins, L. M. and Smith, A. B. *J. Natl. Cancer Inst.* 57 (1976) 841.
7. Kidani, Y., Inagaki, K. and Tsukagoshi, S. *Gann* 67 (1976) 921.
8. Borch, G., Nielsen, P. H. and Klæboe, P. *Acta Chem. Scand. A* 31 (1977) 109.
9. Borch, G., Klæboe, P. and Nielsen, P. H. *Spectrochim. Acta A* 34 (1978) 87.
10. Borch, G., Gustavsen, J., Klæboe, P. and Nielsen, P. H. *Spectrochim. Acta A* 34 (1978) 93.
11. Marumo, F., Utsumi, Y. and Saito, Y. *Acta Crystallogr. B* 26 (1970) 1492.
12. Sudmeier, J. L. and Reilly, C. N. *Anal. Chem.* 36 (1964) 1707.
13. Delépine, M. *Bull. Chim. Soc. Fr.* [5] 1 (1934) 1256.
14. Andersen, P., Galsbøl, F., Harnung, S. E. and Laier, T. *Acta Chem. Scand.* 27 (1973) 3973.
15. Sidgwick, N. V. *The Chemical Elements and their Compounds*, Clarendon Press, Oxford 1950, Vol. I, XXIX.
16. Miyamae, H., Sato, S. and Saito, Y. *Acta Crystallogr. B* 33 (1977) 3391.
17. Kuroda, R., Sasaki, Y. and Saito, Y. *Acta Crystallogr. B* 30 (1974) 2053.
18. Galsbøl, F. *Acta Chem. Scand. A* 32 (1978) 757.
19. Wiberg, K. B. and Shrake, A. *Spectrochim. Acta A* 29 (1973) 583.
20. Snyder, R. G. and Schachtschneider, J. H. *Spectrochim. Acta* 21 (1965) 169.
21. Schmidt, K. H. and Müller, A. *Inorg. Chem.* 14 (1975) 2183.
22. Berg, R. W. and Rasmussen, K. *Spectrosc. Lett.* 4 (8) (1971) 285.
23. Baranovskii, I. B. and Mazo, G. Ya. *Russ. J. Inorg. Chem.* 20 (1975) 244.
24. James, D. W. and Nolan, M. J. *Inorg. Nucl. Chem. Lett.* 9 (1973) 319.
25. Pickett, H. M. and Strauss, H. L. *J. Chem. Phys.* 53 (1970) 376.

Received June 28, 1978.